Conformational Studies by Dynamic NMR. 64.[1] Stereomutations of Atropisomers and of Conformational Enantiomers in Ethers of Hindered Naphthylcarbinols†

Daniele Casarini,* Lodovico Lunazzi,* and Andrea Mazzanti[2]

Department of Organic Chemistry "A. Mangini", University of Bologna, Risorgimento, 4, Bologna 40136, Italy

Elisabetta Foresti

Chemistry Department "G.Ciamician", University of Bologna, Via Selmi, Bologna, Italy

Received March 13, 1998

Methyl or ethyl ethers of 1-naphthyl carbinols $ArCR_2OR'$ (Ar = 1-naphthyl, R′ = Me, Et) can occur in a range of rotational conformations whose population varies with the nature of the substituents R. The passage between such conformation minima is achieved by rotation, during which one group R or OR′ passes either the 2- or the 8-position of the naphthalene, and depending on the nature of R and OR′, some of these interconversions are slow on the NMR time scale. Dynamic NMR experiments, supported by molecular mechanics calculations, show that different minima are preferred as the R group changes. These conformations are identified, their populations are determined, and the barriers to their interconversions are measured. In particular when R is a *tert*-butyl group, two atropisomers (with the OMe moiety near the 2- or 8-position) could be physically separated and their structures determined by NOE experiments in solution and X-ray diffraction in the solid state. Each of these exists as a pair of stereolabile enantiomers, with a barrier of 9−10 kcal mol^{-1} for interconversion.

Introduction

Naphthyldialkylmethanols ($ArCR_2OH$, Ar = 1-naphthyl) exist as a pair of atropisomers having the OH moiety directed either toward position 2 or toward position 8 of the naphthalene ring: they are referred to as anti-periplanar (ap) and syn periplanar (sp), respectively.[3] When the R groups are bulky *tert*-butyl substituents, these atropisomers are amenable to physical separation because the corresponding interconversion barrier is quite high.[3] In the case of smaller R groups, the presence of such atropisomers could only be detected by low-temperature NMR spectroscopy. These results are in agreement with the conformational behavior of similarly hindered carbinols.[4]

Replacement of the OH by a bulkier alkoxy group (OR′) might substantially modify the conformational preferences of these derivatives in that it would destroy, in the ethers, the molecular plane of symmetry which coincides, in the carbinols, with the naphthalene plane. As a consequence it could be anticipated that, contrary to the case of carbinol derivatives, the corresponding ethers will display a pair of stereolabile enantiomers, due to the OR′ moiety adopting a tilted conformation. Accordingly, each of the two atropisomers would consist, in principle, of a racemic mixture of M and P conformational enantiomers (see, for instance, Scheme 1) that should reveal their existence, at appropriate low temperatures, by the breaking of the molecular symmetry. To verify such a prediction, a number of methyl or ethyl ethers (**1**−**7**), derived from 1-naphthyl carbinols ($ArCR_2OH$), have been synthesized and investigated by variable temperature NMR spectroscopy.

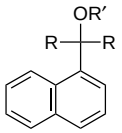

1: R′ = Me, R = Bu–*t*
2: R′ = Me, R = Pr–*i*
3: R′ = Me, R = CH_2Pr^i
4: R′ = Me, R = Et
5: R′ = Me, R = Me
6: R′ = Et, R = Et
7: R′ = Et, R = Me

Results and Discussion

(a) Di-*tert*-butyl-α-naphthylmethyl Methyl Ether (1). When alkylated with methyl iodide (see Experimental Section) the sp and ap atropisomers of the carbinol $ArC(Bu^t)_2OH$ (Ar = 1-naphthyl) [3] yield the corresponding atropisomers of **1**. In contrast with the parent carbinols, one of them is stable both in the solid and in solution (**1-A**) while the other one (**1-B**) is stable only in the solid state and interconverts completely into **1-A** when solvents are added. The sp and ap structures (Scheme 2) were assigned to **1-A** and **1-B**, respectively, by means of difference NOE experiments.

† Respectfully dedicated to the memory of Professor Antonino Fava, 1923−1997.

(1) For Part 63, see: Cerioni, G.; Cremonini, M. A.; Lunazzi, L.; Placucci, G.; Plumitallo, A. *J. Org. Chem.* **1998**, *63*, 3933.

(2) In partial fulfilment of the Ph.D. requirements in Chemical Sciences, University of Bologna.

(3) Casarini, D.; Lunazzi, L.; Mazzanti, A. *J. Org. Chem.* **1997**, *62*, 3315.

(4) (a) Newsoroff, G. P.; Sternhell, S. *Tetrahedron Lett.* **1967**, 2539. (b) Baas, J. M. A.; van der Toorn, J. M.; Wepster, B. M. *Rec. Trav. Chim. Pays-Bas* **1974**, *93*, 133. (c) Lomas, J. S.; Luong, P. K.; Dubois, J.-E. *J. Org. Chem.* **1977**, *42*, 3394. (d) Lomas, J. S.; Anderson, J. E. *J. Org. Chem.* **1995**, *60*, 3246.

S0022-3263(98)00480-0 CCC: $15.00
Published on Web 06/18/1998

Scheme 1. Schematic Representation of the M and P Enantiomers for the sp and for the ap Atropisomers of 1 (R = *t*-Bu, R′ = Me)

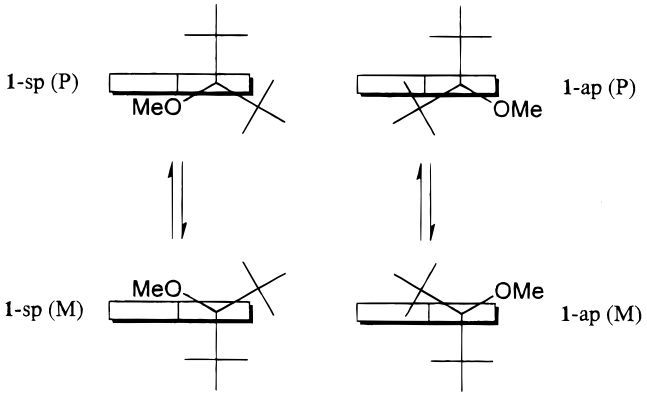

Scheme 2. MM-Computed Structures (top) of the sp and ap Atropisomers of 1 (Left and Right, Respectively). Underneath Is Reported the Experimental (X-ray) Structure of 1-A

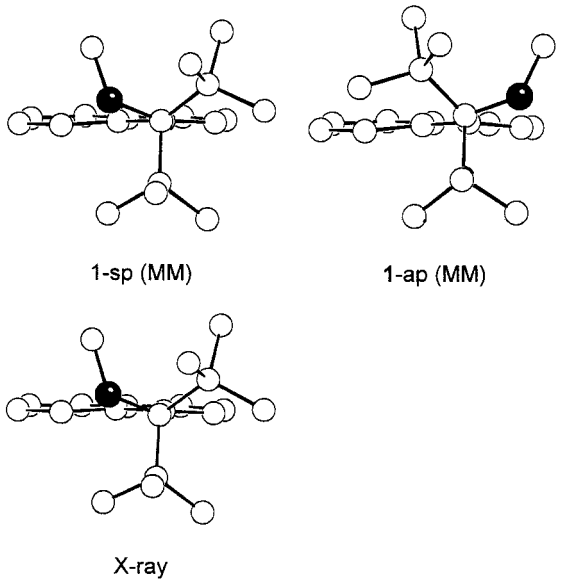

In the case of **1-A** irradiation of the ^{1}H line of the MeO group enhances only the H-8 signal (11%), whereas irradiation of the *tert*-butyl line enhances the H-2 more than the H-8 signal (31% vs 18%). Conversely irradiation of the MeO line of **1-B** (this experiment was performed by keeping the solution below −10 °C to avoid interconversion into **1-A**) enhances solely the H-2 signal (9%) whereas irradiation of the *tert*-butyl line enhances the H-8 more than the H-2 signals (43% vs 11%). As observed in the corresponding carbinols, the H-8 shift of the sp atropisomer is downfield with respect to that of the ap atropisomer (8.9 and 8.5 ppm, respectively). This feature was also used to assign the sp and ap structures in similar derivatives of this series.

The kinetics of the process which interconverts the less stable ap (**1-B**) into the more stable sp atropisomer (**1-A**) yields a first-order rate constant of 9.9×10^{-5} s^{-1} (in $CDCl_3$ at 45 °C), corresponding to a free energy of activation ($\Delta G^{\ddagger}$) of 24.4 kcal mol^{-1} (Table 1). This value is somewhat lower than that (29.9 kcal mol^{-1}) measured for the analogous interconversion of the corresponding less stable into the most stable carbinol.[3]

Table 1. Barriers ($\Delta G^{\ddagger}$, kcal mol^{-1}) for the Interconversion of the Atropisomers in 1−3 and for the C−R Rotation of the *tert*-Butyl (in 1-sp and 1-ap) and Isopropyl (in 2-sp) Groups

compd	$\Delta G^{\ddagger}$	compd	$\Delta G^{\ddagger}$
1	24.4[a]	**1**-sp	8.5[c]
2	13.2[b] (11.6)[a]	**1**-ap	9.8[c,d]
3	11.9[b] (11.1_5)[a]	**2**-sp	8.0[e] 11.1[e]

[a] Interconversion of the atropisomer ap (less stable) into sp (more stable). [b] Interconversion of the atropisomer sp (more stable) into ap (less stable). [c] C−Bu^t rotation. [d] Rotation correlated with enantiomerization (see text and Table 2). [e] C−Pr^i rotation (gear effect).

Molecular mechanics (MM) calculations[5] predict indeed that the **1**-ap atropisomer is much less stable (its computed relative energy is 6.2 kcal mol^{-1} higher) than the **1**-sp atropisomer, so experiment and calculations agree in accounting for the disappearance of the ap atropisomer (**1-B**) at equilibrium in solution. These calculations also indicate that the transition state for the **1**-ap to **1**-sp interconversion corresponds to the passage of the methyl groups of one *tert*-butyl moiety past the position 8 of the naphthalene ring.[6] The barrier computed in this way (23.8 kcal mol^{-1}) is very close to that (24.4 kcal mol^{-1}) determined experimentally.

The MM-computed structures of Scheme 2 indicate that both atropisomers adopt asymmetric conformations, having the MeO moiety tilted with respect to the naphthalene plane by dihedral angles of 25° (**1**-sp) or 21° (**1**-ap). As a consequence both **1**-sp and **1**-ap should display diastereotopic *tert*-butyl groups, one of them being essentially orthogonal to the naphthalene plane and the other forming a dihedral angle of about 40°.

A single-crystal X-ray diffraction of the more stable atropisomer **1-A** showed that the O−C−C(1)−C(9) dihedral angle is 22°, thus confirming the syn periplanar structure indicated by the NOE experiments in solution. The MM calculations, predicting an angle of 25°, appear therefore quite reliable and make, as a consequence, very plausible the structure computed for atropisomer **1-B** that was not investigated by X-ray diffraction (we were unable to grow single crystals of **1-B** from its solutions owing to the rapid interconversion into **1-A**).

The existence of the M and P enantiomers, generated by the Ar−CO stereogenic axis (Scheme 1), is made evident by the X-ray diffraction showing how the unit cell of **1-A** contains three independent molecules, two of which have *opposite chirality* (see Experimental Section). In other words **1-A** crystallizes as an "anomalous racemate" having a 2:1 molecular combination, i.e., half of the crystals have a M_2P and half a P_2M composition.[7]

In solution these enantiomers are stereolabile, owing to the fast M−P interconversion, but their presence can be inferred at appropriate low temperatures by taking advantage of the symmetry breaking due to the decelera-

(5) Use was made of the programs GMMX (for searching the conformational minima) and PC MODEL (employing the MMX force field), as implemented by Serena Software, Bloomington, IN.

(6) This situation corresponds to a rotational transition state where the C(9)−C(1)−C(O)−C(Me_3) dihedral angle (i.e., the angle formed by *tert*-butyl with the naphthalene ring) is 33°, a result analogous to that reported for a similar case in Anderson, J. E.; Barkel, D. J. D. *J. Chem. Soc., Perkin Trans. 2* **1984**, 1053.

(7) Jacques, J.; Collet, A.; Wilen, S. H. *Enantiomers, Racemates, and Resolutions*; Wiley: New York, 1981; p 147.

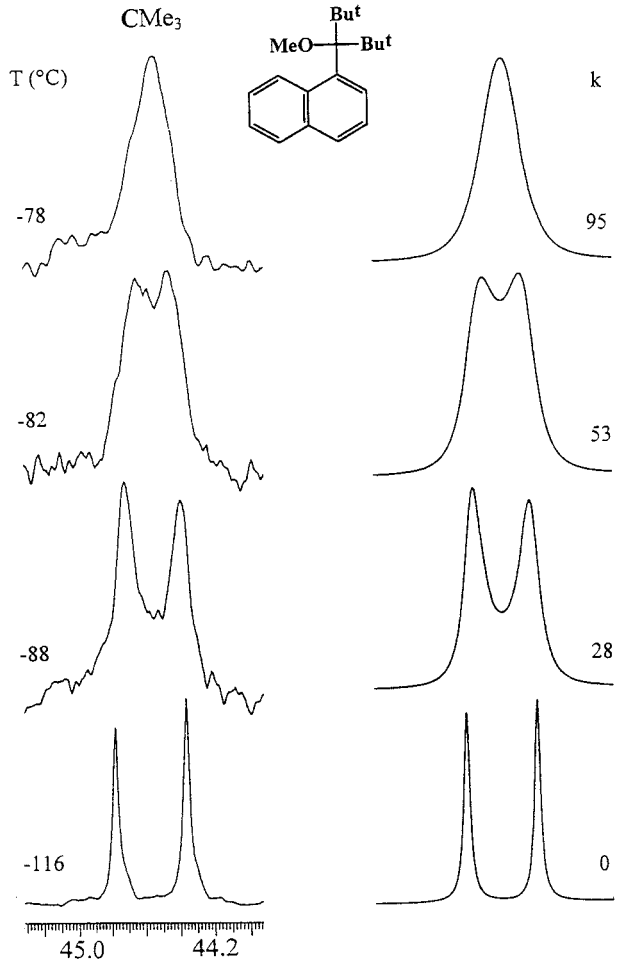

Figure 1. Experimental (left) ^{13}C spectrum (100.6 MHz in CHF_2Cl/CD_2Cl_2) of the quaternary carbons of the *tert*-butyl substituents of **1**-sp as function of temperature. These groups become diastereotopic at low temperature, indicating the presence of M and P conformational enantiomers. On the right are reported the simulated spectra obtained with the rate constants (k, in s^{-1}) indicated.

Table 2. Barriers ($\Delta G^{\ddagger}$, kcal mol^{-1}) for the M−P Enantiomerization in the sp Atropisomers of 1−7 and in the ap Atropisomer of 1

compd	$\Delta G^{\ddagger}$	compd	$\Delta G^{\ddagger}$
1-sp	9.3	**4**-sp	9.2
1-ap	9.8[a]	**5**-sp	7.2
2-sp	9.7	**6**-sp	9.7
3-sp	9.3	**7**-sp	7.5

[a] Motion correlated with the *tert*-butyl rotation (see text and Table 1).

tion of the enantiomerization rate. Whereas the ^{13}C line of the OMe group is a sharp singlet at any temperature (and likewise the remaining singlets of the carbon signals of the naphthalene moiety), that due to the pair of quaternary *tert*-butyl carbons broadens and eventually splits into a 1:1 doublet below −82 °C (Figure 1). Line shape simulation affords the rate constants for interconverting the M and P stereolabile enantiomers of **1-A**, the corresponding process having $\Delta G^{\ddagger} = 9.3$ kcal mol^{-1} (Table 2).

Since in these enantiomers the *tert*-butyl substituents are diastereotopic, also their methyl groups would give rise to a pair of NMR signals. However, the situation is further complicated, in practice, by the occurrence of a restricted rotation about the C−CMe_3 bonds, which makes the ^{13}C single signal of the six equivalent methyl groups split into six lines at −115 °C. At intermediate temperatures (between −80 and −90 °C) three lines appear to be much sharper than the other three, indicating that the two *tert*-butyl groups rotate at different rates. As a consequence the line shape simulation of these signals requires, in principle, three sets of rate constants i.e., a k_1 to account for the enantiomerization (which must coincide with that determined by monitoring the lines of the quaternary carbons) and two rate constants (k_2 and k_3) to account for the internal rotation of the two diastereotopic *tert*-butyl groups.

A satisfactory spectral simulation could only be achieved by keeping one of the two rotational constants (e.g., k_3) always equal to zero. The set of k_1 values obtained at various temperatures provided $\Delta G_1^{\ddagger} = 9.3$ kcal mol^{-1} for the enantiomerization process (a value equal to that obtained from the spectra of the quaternary carbons), and the set of k_2 values yielded $\Delta G_2^{\ddagger} = 8.5$ kcal mol^{-1}, which corresponds to the rotational barrier of *only one* of the two *tert*-butyl groups. Essentially the same results were obtained from the ^1H spectra reported in Figure 2 (left), where the six methyl groups yield five signals at −118 °C, two being accidentally coincident (the integrated area of the upfield signal is in fact twice as large). The $\Delta G_1^{\ddagger}$ and $\Delta G_2^{\ddagger}$ values for the enantiomerization and for the rotation of one of the two *tert*-butyl groups were found to be, respectively, 9.2 and 8.3 kcal mol^{-1}, the difference with respect to the ^{13}C figures lying within the experimental errors (±0.2 kcal mol^{-1}).

The coinciding results of these two NMR experiments imply that when the enantiomerization process (brought about by the rotation about the Ar−CO chirality axis) is slow and the two *tert*-butyl groups thus begin to become diastereotopic, one of them still rotates with a measurable rate whereas the other is already locked in a fixed position. Within the latter group the three methyls do not exchange by direct rotation about the C−CMe_3 bond because this is too hindered a process in the position now occupied by this *tert*-butyl: a circumstance which justifies the null values for k_3.

At higher temperatures these three lines appear to exchange, but they manage to do so through an alternative pathway. In fact the enantiomerization process occurring with the rate k_1 brings this *tert*-butyl into the position of its companion, where a less hindered environment allows it to rotate with the very same rate k_2. When the enantiomerization equilibrium brings this *tert*-butyl back into its previous (hindered) position, the three methyl groups have exchanged their sites by making use of the rate constants k_1 and k_2. A similar situation, related to the motions of a different molecule, has been recently described.[8]

Inspection of the X-ray and MM structures of **1**-sp (Scheme 1, left) suggests that the *tert*-butyl group perpendicular to the naphthalene plane should be the one allowed to undergo the direct rotation process (i.e., that corresponding to a $\Delta G_2^{\ddagger} = 8.3-8.5$ kcal mol^{-1}) whereas the other should follow the two-step pathway. This is because the environment of the latter appears to be more sterically demanding than that of its companion.

(8) Anderson, J. E.; Casarini, D.; Lunazzi, L. *J. Org. Chem.* **1996**, *61*, 1290.

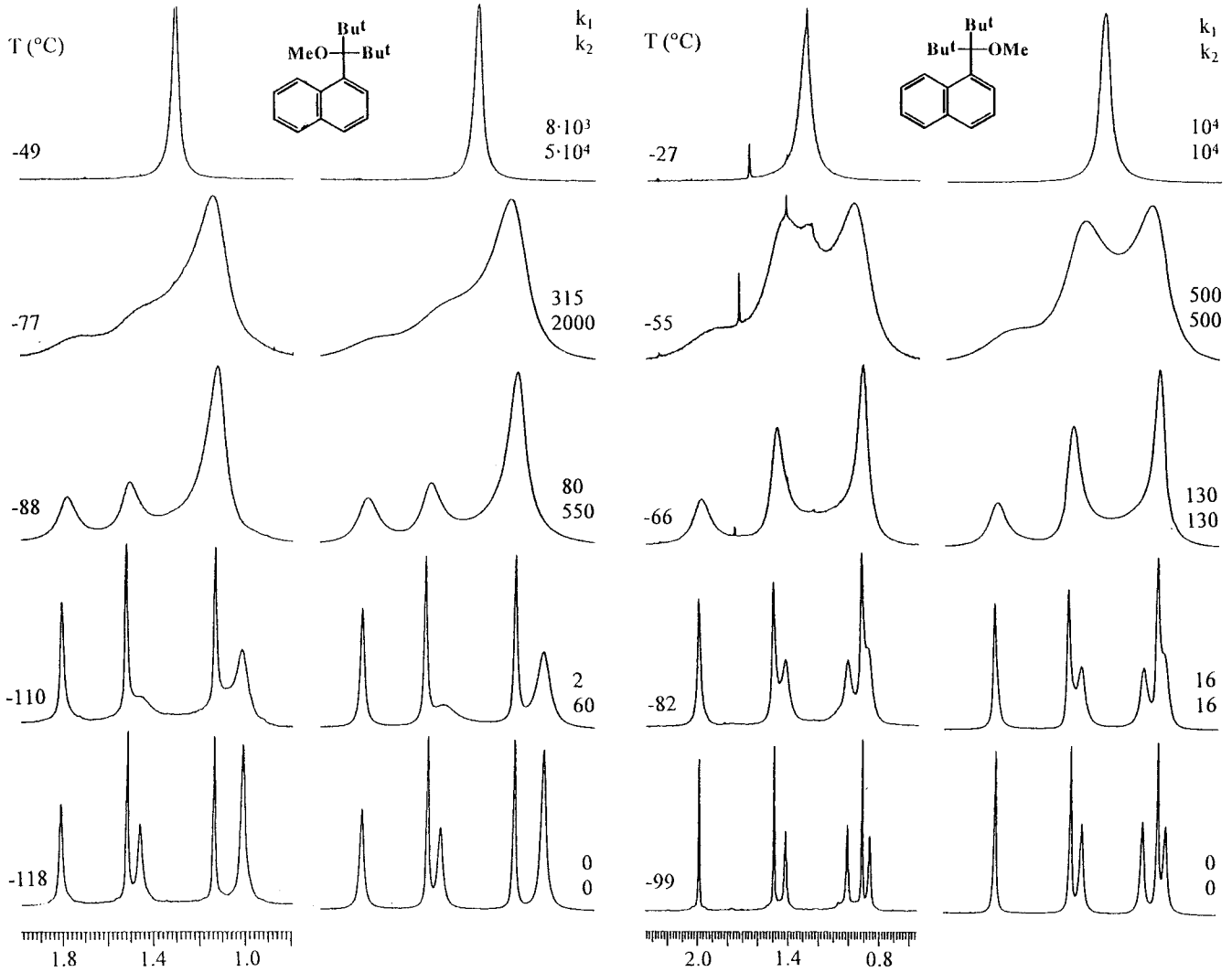

Figure 2. ^{1}H experimental and simulated 300 MHz spectra of the methyl groups of the *tert*-butyl substituents of the **1**-sp atropisomer in $CBrF_3/CD_2Cl_2$ (left) and of the **1**-ap atropisomer in CD_2Cl_2 (right) as function of temperature. Both the M−P enantiomerization and the *tert*-butyl rotation processes become slow on lowering the temperature, thus yielding six lines for the six methyl groups (the two upfield lines of **1**-sp are accidentally coincident). The rate constants k_1 and k_2 (in s^{-1}) used for the simulation are also reported, k_3 being always equal to zero (see text).

The interpretation we offered for these motions requires that below −90 °C the M and P enantiomers of the **1**-sp atropisomer should be sufficiently long lived to display different NMR spectra in a chiral environment. Actually the ^{1}H line of the OMe group, recorded in the presence of a molar excess (e.g., 20:1) of an enantiomerically pure Pirkle alcohol (TFAE),[9] broadens on lowering the temperature below −70 °C and splits at −100 °C into a 1:1 doublet (a few other lines of **1-A** split likewise, as expected). Line shape simulation of the OMe doublet as a function of temperature affords the same $\Delta G_1^{\ddagger}$ value of 9.3 kcal mol^{-1} for the enantiomerization, as determined by monitoring the quaternary *tert*-butyl carbon ^{13}C line in an achiral environment.

Similar results concerning the molecular motions were obtained in the case of the less stable ap atropisomer **1-B**. Again the ^{13}C line of the quaternary *tert*-butyl carbons, which appears as a sharp singlet at −20 °C, broadens and then splits at −90 °C into a 1:1 doublet with an M/P enantiomerization barrier ($\Delta G^{\ddagger}$ = 9.8 kcal mol^{-1}) which is 0.5 kcal mol^{-1} higher than that of the sp atropisomer (Table 2). The ^{13}C single signal of the six *tert*-butyl methyl groups splits into five lines at −100 °C (two of them accidentally coincide) as does the ^{1}H line which, at the same temperature, displays all six lines expected for the six different methyl groups (see Figure 2, right). As in the case of **1**-sp the line shape simulation was performed with a set of enantiomerization rate constants (k_1) which yields a $\Delta G_1^{\ddagger}$ (9.8 kcal mol^{-1}) equal to that previously determined from the quaternary carbons line. Again one of the two sets of the *tert*-butyl rotation rate constants (k_3) turned out to be zero at any temperature. The values of the other *tert*-butyl rotation rate constants k_2, on the other hand, were found to be essentially equal to those of the enantiomerization rate constant (k_1) at the same temperatures, hence yielding an equal $\Delta G^{\ddagger}$ value (i.e., 9.8 kcal mol^{-1}).[10] This result implies that in **1**-ap such a rotation is not independent of enantiomer-

(9) TFAE corresponds to (*S*)-*d*-2,2,2-trifluoro-1-(9-anthryl)ethanol. See: Pirkle, W. H. *J. Am. Chem. Soc.* **1966**, *88*, 1837.

(10) Acceptable spectral simulations could be obtained even assuming slightly different k_1 and k_2 rate constants. Such small differences, however, yielded $\Delta G_1^{\ddagger}$ and $\Delta G_2^{\ddagger}$ values separated by less than 0.2 kcal mol^{-1}. Within the experimental uncertainty (±0.2 kcal mol^{-1}) they are therefore indistinguishable.

ization in that the two motions are strongly correlated, thus sharing a common transition state[11] (the alternative hypothesis of two independent barriers being equal by sheer chance seemed untenable to us). The negligible values for k_3 can be explained in the same way as in the previous case: one of the two diastereotopic *tert*-butyl groups of **1**-ap can rotate only when the enantiomerization process brings it to visit the less hindered site of its companion, the only difference being that now the rotation of the latter occurs through a common pathway with the enantiomerization process.

The barriers for the C−CMe_3 rotation are in a range similar to that reported for analogous *tert*-butyl derivatives.[3,12]

The M/P enantiomerization of **1** has been also investigated by MM methods. In the case of the more stable **1**-sp atropisomer, this barrier was calculated as the difference between the ground state and a transition state where the OMe group passes over position 8 of the naphthalene ring. In doing so the OMe group also rotates about the C−OMe bond and accommodates itself in the C(9)−C(1)−C(O) plane with a MeO−C−C(1) dihedral angle of 180° in order to minimize the interaction with H-8. The barrier computed with such a model (9.7 kcal mol^{-1}) matches satisfactorily the experimental value of 9.3 kcal mol^{-1}.

An analogous approach was followed for the **1**-ap atropisomer where the OMe group passes over position 2 of naphthalene: likewise the OMe group lies in the C(2)−C(1)−C(O) plane with a MeO−C−C(1) dihedral angle of 180°. The computed barrier (8.7 kcal mol^{-1}) however is lower than that computed for **1**-sp, whereas the experimental value is larger (9.8 vs 9.3 kcal mol^{-1} for **1**-ap and **1**-sp, respectively). The reversal of the computed with respect to the experimental trend seems to lend some support to the hypothesis that the enantiomerization is not an isolated process in **1**-ap as it is in **1**-sp. In fact the simple model which we employed to describe the isolated enantiomerization process is adequate for the case of **1**-sp but obviously inadequate to properly describe a situation where two motions are effectively correlated, as in **1**-ap.

(b) Diisopropyl-α-naphthylmethyl Methyl Ether (2). The conformational situation of the isopropyl is more complicated than that of the *tert*-butyl derivative since the molecule is more flexible, due to the lower steric requirements. The smaller dimensions of the two isopropyl substituents allow a more facile interconversion of the two atropisomers, so that they could not be isolated as in the case of **1**. However, many ^1H and ^{13}C NMR signals of **2** showed at low temperature (about −50 °C) the presence of two conformers of different structure and stability: the ^{13}C line of the OMe group was most informative for this purpose (Figure 3).

The singlet observed at room temperature broadens on cooling, reaching a maximum width at about −32 °C.[13]

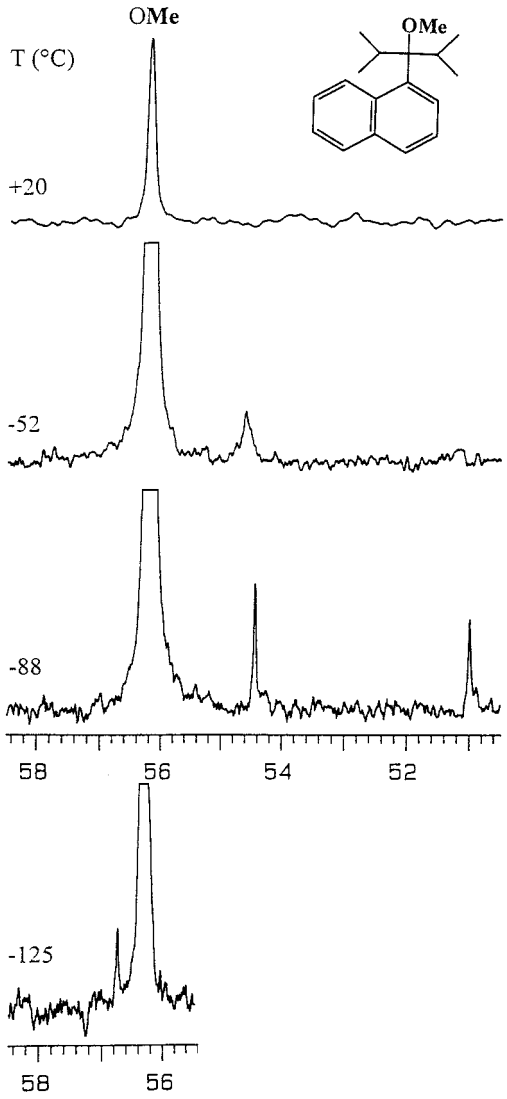

Figure 3. ^{13}C signal (75.5 MHz in CHF_2Cl/C_6D_6) of the OMe group of **2** at three temperatures (top) showing the subsequent appearance of two minor peaks. Underneath is reported the ^{13}C spectrum (100.6 MHz in CHF_2Cl/CD_2Cl_2) at an even lower temperature (−125 °C) displaying a third additional minor peak (see text).

The signal sharpens again on further cooling to reveal a second peak[14] (about 3%) at −55 °C, with a shift which is 1.7 ppm upfield with respect to the major one (Figure 3). From the line shape analysis a $\Delta G^{\ddagger}$ value of 12.9 ± 0.3 kcal mol^{-1} was obtained for this exchange. This process corresponds to the equilibrium between the atropisomers **2**-sp and **2**-ap of Scheme 3, as determined on the basis of the corresponding ^1H signals of the hydrogens in position 8. At −55 °C, in fact, the more intense signal (97%) displays a H-8 shift (9.02 ppm) diagnostic of a sp atropisomer, the weaker one (3%) a shift (8.25 ppm) typical for an ap atropisomer. Line shape analysis of the latter pair of signals (recorded at 600 MHz for better accuracy) yielded a $\Delta G^{\ddagger}$ value (13.2 ± 0.2 kcal mol^{-1}, Table 1) equal, within the errors, to that previously determined.

(11) (a) Berg, U.; Liljefors, T.; Roussel, C.; Sandström, J. *Acc. Chem. Res.* **1985**, *18*, 80. (b) Berg, U.; Sandström, J. *Adv. Phys. Org. Chem.* **1989**, *25*, 1. (c) Anderson, J. E. In *The Chemistry of Alkanes and Cycloalkanes*; Patai, S., Rappoport, Z., Eds.; Wiley: London, 1992; Chapter 3, p 95. (d) Rappoport, Z.; Biali, S. E. *Acc. Chem. Res.* **1997**, *30*, 307.

(12) (a) Hoogasian, S.; Bushweller, C. H.; Anderson. W. G.; Kingsley, G. *J. Phys. Chem.* **1976**, *80*, 643. (b) Anderson J. E.; Kirsch, P. A.; Lomas, J. S. *J. Chem. Soc., Chem. Commun.* **1988**, 1065. (c) Riddell, F. G.; Arumugam, S.; Anderson, J. E. *J. Chem. Soc., Chem. Commun.* **1991**, 1525. (d) Barrie, P. J.; Anderson, J. E. *J. Chem. Soc., Perkin Trans. 2* **1992**, 2031.

(13) (a) Anet, F. A. L.; Yavari, I.; Ferguson, I. J.; Katritzky, A. R.; Moreno-Manas, R.; Robinson, M. J. T. *J. Chem. Soc., Chem. Commun.* **1976**, 399. (b) Sandström, J. *Dynamic NMR Spectroscopy*; Academic Press: London, 1982; p 84.

(14) (a) Griendley, T. B. *Tetrahedron Lett.* **1982**, *23*, 1757. (b) Lunazzi, L.; Placucci, G.; Macciantelli, D. *Tetrahedron* **1991**, *47*, 6434.

Scheme 3. Schematic Representation of the Two Atropisomers of 2. The MM-Computed Relative Energies (*E*) Are in kcal mol^{-1}

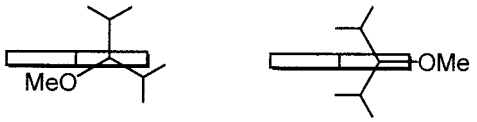

2-sp (E = 0) **2**-ap (E = 1.85)

Molecular mechanics calculations actually predict that the **2**-sp atropisomer should be 1.85 kcal mol^{-1} more stable than the **2**-ap atropisomer (Scheme 3). Such an energy difference entails a population of the latter equal to 1.5% at −55 °C, in satisfactory agreement with experiment (about 3% at the same temperature).

When the temperature is lowered below −55 °C, the ^{13}C signal of the OMe moiety first broadens and subsequently sharpens again, eventually revealing (at −88 °C) a second minor upfield line (about 2.5%) which is even more separated ($\Delta\delta$ = 5.05 ppm) from the major one (Figure 3). Such an occurrence indicates that a second motion has been rendered slow on the NMR time scale with a barrier (derived from line shape analysis) equal to 11.1 ± 0.2 kcal mol^{-1} (Table 1).

When the sample is further cooled below −90 °C, a third dynamic process become observable, giving rise to a third minor ^{13}C signal (about 10% at −125 °C) which, as shown in Figure 3, appears downfield ($\Delta\delta$ = 0.55 ppm) with respect to the major OMe peak (the normalized ratio for the three conformers of **2**-sp is therefore 2:9:89). Line shape analysis yielded a $\Delta G^{\ddagger}$ value equal to 8.0 ± 0.2 kcal mol^{-1} for this third motion (Table 1).

The two fastest processes detected by monitoring the ^{13}C OMe line (i.e., those with $\Delta G^{\ddagger}$ = 11.1 and 8.0 kcal mol^{-1}) are a manifestation of the so-called "gear effect" which is often observed when two isopropyl groups are bonded to the same or neighboring atoms.[15,16] The interplay between two such isopropyl substituents generates "gear-conformers" which interconvert into each other with barriers ($\Delta G^{\ddagger}$ values in the range 6.5−17.0 kcal mol^{-1})[16−18] higher than that expected for the isolated rotation of an isopropyl group.[19] Although four such rotational conformers (rotamers) can be in principle predicted, only two,[16,17] and occasionally three,[18] have been, in practice, observed.

The MM calculations indicates that the atropisomer **2**-sp has indeed three energy minima, which only differ for the relative positions adopted by the pair of isopropyl substituents: they are displayed in Scheme 4 and labeled **2**-sp$_a$, **2**-sp$_b$, and **2**-sp$_c$.

Scheme 4. MM-Computed Structures of the Three Gear Rotamers of 2-sp. The Experimental Barriers (ΔG^*) and the Computed Relative Energies (*E*) Are in kcal mol^{-1}

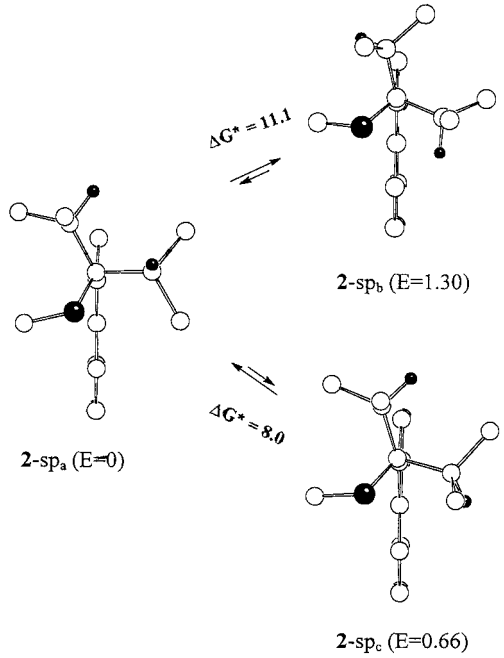

The energy difference between the rotamers **2**-sp$_a$ and **2**-sp$_b$ (1.3 kcal mol^{-1}) corresponds to a ratio (97:3 at −88 °C) in agreement with the population (2.5%) observed at the same temperature. On this basis conformation **2**-sp$_b$ should be assigned to the rotamer having its OMe line 5.05 ppm upfield with respect to that of the major rotamer **2**-sp$_a$. According to this assignment the experimental barrier of 11.1 kcal mol^{-1} should correspond to the interconversion of **2**-sp$_a$ into **2**-sp$_b$.

The energy minimum of the rotamer **2**-sp$_c$ is 0.66 kcal mol^{-1} higher than that of **2**-sp$_a$, which entails a 90:10 ratio at −125 °C, in agreement with the values detected at the same temperature for the rotamer having the OMe line 0.55 ppm downfield to that of the major one (**2**-sp$_a$). The corresponding experimental barrier (8.0 kcal mol^{-1}) should thus be assigned to the interconversion of **2**-sp$_a$ into **2**-sp$_c$. The experimental spectra do not show any evidence of a direct exchange between the two minor rotamers (when each of the corresponding weak lines broadens, in fact, the other remains sharp), thus suggesting that they do not interconvert directly into each other but only through the intermediacy of the major rotamer **2**-sp$_a$ (Scheme 4). This conclusion is the same as that reported for other cases where the exchange involving three such rotamers was found to occur, likewise, via a two barrier pathway.[13b,18]

As shown in Scheme 3, the **2**-sp atropisomer is predicted to have an asymmetric, thus chiral, conformation since the OMe group is tilted away (by 21°) from the naphthalene plane. Accordingly, if the motion of the OMe group above and below such a plane is rendered slow on the NMR time scale, the resulting M and P conformational enantiomers will be sufficiently long lived to display diastereotopic isopropyl substituents. On the contrary the **2**-ap atropisomer is expected to be achiral,

(15) (a) Roussel, C.; Chanon, M.; Metzger, J. *Tetrahedron Lett.* **1971**, 1861. (b) Siegel, J.; Gutiérrez, A.; Schweizer, W. B.; Ermer, O.; Mislow, K. *J. Am. Chem. Soc.* **1986**, *108*, 1569. (c) Columbus, I.; Biali, S. E. *J. Org. Chem.* **1994**, *59*, 3402.

(16) (a) Bomse, D. S.; Morton, T. H. *Tetrahedron Lett.* **1975**, 781. (b) Ermer, O. *Angew. Chem., Int. Ed. Engl.* **1983**, *22*, 998. (c) Cerioni, G.; Piras, P.; Marongiu, G.; Macciantelli, D.; Lunazzi, L. *J. Chem. Soc., Perkin Trans. 2* **1981**, 1449. (d) Lunazzi, L.; Guerra, M.; Macciantelli, D.; Cerioni, G. *J. Chem. Soc., Perkin Trans. 2* **1982**, 1527. (e) Pettersson, I.; Berg, U. *J. Chem. Soc., Perkin Trans. 2* **1985**, 1365. (f) Anderson, J. E.; Bettels, B. R. *Tetrahedron Lett.* **1986**, *27*, 3909.

(17) (a) Roussel, C.; Lidén, A.; Chanon, M.; Metzger, J.; Sandström, J. *J. Am. Chem. Soc.* **1976**, *98*, 2847. (b) Berg, U.; Roussel, C. *J. Am. Chem. Soc.* **1980**, *102*, 7848. (c) Bartoli, G.; Bosco, M.; Lunazzi, L.; Macciantelli, D. *Tetrahedron Lett.* **1994**, *50*, 2561.

(18) (a) Lidén, A.; Roussel, C.; Liljefors, T.; Chanon, M.; Carter, R. E.; Metzger, J.; Sandström, J. *J. Am. Chem. Soc.* **1976**, *98*, 2853. (b) Liljefors, T.; Sandström, J. *Org. Magn. Reson.* **1977**, *9*, 276.

(19) The barrier for an isolated C−Pr^i rotation was found to be as low as 4.3 kcal mol^{-1} (Lunazzi, L.; Macciantelli, D.; Bernardi, F.; Ingold, K. U. *J. Am. Chem. Soc.* **1977**, *99*, 457).

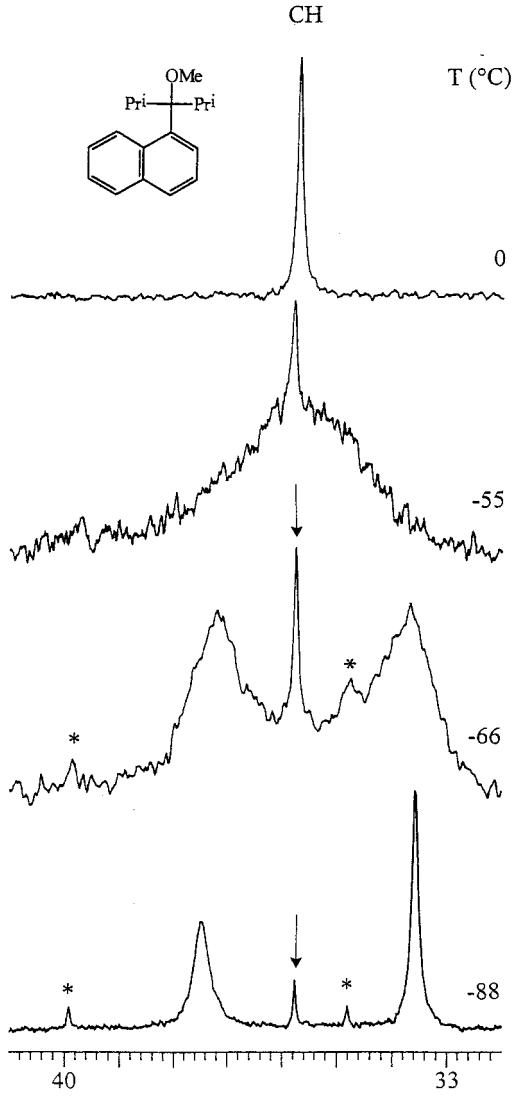

Figure 4. ^{13}C spectrum (75.5 MHz in CHF_2Cl/C_6D_6) of the isopropyl CH line of **2** as function of temperature. Five peaks are detectable at −88 °C: the more intense and the less intense (starred) pairs are diagnostic of two chiral atropisomers, the single peak (arrowed) of a symmetric (achiral) atropisomer.

having the OMe group on the same plane of the naphthalene ring.

Both such predictions were verified by monitoring the ^{13}C signals of the isopropyl CH carbons of compound **2**.

At room temperature these carbons display a single sharp peak which splits, at −55 °C (Figure 4), into a weak sharp line and into an intense broad signal. This is because the interconversion of **2**-sp into **2**-ap has become slow, as already observed when the OMe and H-8 signals were monitored. The weak line, which belongs to the **2**-ap atropisomer, never broadens, nor splits at any attainable temperature (well below −100 °C). This indicates that the two isopropyl groups are enantiotopic, as expected for the symmetric conformation of Scheme 3.

On the contrary, the intense broad signal of the major **2**-sp atropisomer splits into a pair of equally intense lines below −55 °C (Figure 4). This is due to the slow interconversion of the M and P enantiomers expected for the chiral conformation of Scheme 3, and it is the same type of process observed in **1**-sp when the signals of the quaternary *tert*-butyl carbons of Figure 1 are monitored.

The corresponding $\Delta G^{\ddagger}$ value (9.7 kcal mol^{-1}), derived from a line shape analysis, is quite similar to that found in **1**-sp (9.3 kcal mol^{-1}) in that both processes correspond to the OMe group crossing position 8 of the naphthalene ring.

At temperatures low enough (e.g., at −66 °C and below) as to make sufficiently sharp the two major CH lines, the weak signals (starred in Figure 4) due to the first of the two minor rotamers generated by the gear effect (**2**-sp_b) became also visible,[20] as has already been observed when the OMe (Figure 3) signal was monitored in a similar temperature range. The minor **2**-sp_b rotamer displays two CH signals since, as conceivable, its enantiomerization barrier is similar to that of its major partner **2**-sp_a.

In Figure 4 the downfield peak of the major pair of signals (due to **2**-sp_a) appears much broader than that upfield when the temperature is further lowered (for instance at −88 °C). This is because the process involving the equilibrium with the third rotamer **2**-sp_c begins to slow at lower temperatures, having a barrier (8.0 kcal mol^{-1}) smaller than the other one (11.1 kcal mol^{-1}). Since the shift separation for the CH downfield peaks of **2**-sp_a and **2**-sp_c is larger than for those upfield, the line width of the averaged downfield signal is broader, as predicted by the theory of the exchange.[13b] Eventually the additional peaks of the rotamer **2**-sp_c were also detected at about −120 °C.

The conclusions derived from the above analysis are further confirmed by the ^{13}C spectrum of the isopropyl methyl region. The corresponding signals are, however, even more numerous as these methyl groups are inherently diastereotopic. Thus at −88 °C there are *four* intense and *three* weaker peaks (the *fourth* being overlapped by one of the major lines) for the asymmetric **2**-sp_a and **2**-sp_b rotamers, respectively and, in addition, *two* small peaks for the symmetric **2**-ap atropisomer. At even lower temperatures some of the major lines broaden again as the process involving the third (**2**-sp_c) rotamer decelerates, but the spectrum becomes eventually too crowded to be meaningfully interpreted.

(c) Diisobutyl-α-naphthylmethyl Methyl Ether (3). In the case of R = CH_2Pr^i the conformational behavior is similar to that of **2**, since at low temperature two atropisomers were also detected. The ^1H spectrum shows that the major atropisomer (85%) has the sp structure, because at −60 °C the corresponding H-8 shift is 9.0 ppm whereas that of the minor one is 8.1 ppm. From the line shape analysis of these signals the barrier (11.9 kcal mol^{-1}) to interconversion of **3**-sp into **3**-ap was determined (Table 1). At that temperature also the ^{13}C line of the CH_2 carbon splits into two signals with approximately the same 85:15 ratio, the major one being

(20) To detect the gear rotamers of Scheme 4 (i.e., **2**-sp_a, **2**-sp_b, **2**-sp_c) it is not necessarily required that the adopted conformation is asymmetric (i.e., with the OMe group tilted from the naphthalene ring). They can still be observed even when a rapid M−P enantiomerization process (analogous to that shown in Scheme 1 for R = Bu^t) makes the naphthalene ring an effective dynamic plane of symmetry for **2**-sp (see for instance the case of 1,1-dimethyl-2,2-diisopropylcyclopropane, were the existence of a molecular plane of symmetry does not prevent the detection of two such gear rotamers[16f]). In other words, the enantiomerization and the exchange of these rotamers are independent processes, so that the existence of long lived M and P enantiomers is not a condition for detecting the gear rotamers of Scheme 4. This accounts for the fact that the interconversion barrier of **2**-sp_b into **2**-sp_a is higher (11.1 kcal mol^{-1}) and that of **2**-sp_c into **2**-sp_a is lower (8.0 kcal mol^{-1}) than the M−P enantiomerization barrier (9.7 kcal mol^{-1}).

very broad, the minor very sharp. On further lowering the temperature, the signal of the major **3**-sp atropisomer broadens even more and eventually splits, at −80 °C, into a 1:1 doublet. The barrier measured for this second process (9.3 kcal mol^{-1}) is evidently due to the exchange of the M and P enantiomers of **3**-sp (Table 2). On the contrary the sharp signal of the minor **3**-ap atropisomer does not split, even at −140 °C, indicating that the latter adopts a symmetric conformation. Indeed the MM calculations support this interpretation since the **2**-ap atropisomer has a computed MeO−C−C(1)−C(2) dihedral angle of 0°. On the contrary the MeO−C−C(1)−C(9) dihedral angle computed for the **3**-sp atropisomer is equal to 45°, in agreement with the experimental observation of a chiral conformer. The computed energy difference between the two atropisomers is 1.1 kcal mol^{-1}, corresponding to a ratio (93:7 at −60 °C) reasonably close to the experimental one.

(d) Diethyl-α-naphthylmethyl Methyl Ether (4) and Ethyl Ether (6). Contrary to what that observed in **2** and **3**, the diethyl derivative **4** displays, at any temperature, spectra corresponding to a single atropisomer to which the sp structure was assigned on the basis of the low-temperature H-8 shift value (9.0 ppm at −80 °C). Indeed the MM calculations predict that the energy difference between the **4**-sp and **4**-ap structures is 3.3 kcal mol^{-1}, a value which would entail a population for the minor **4**-ap atropisomer too low (e.g., 0.2% at −80 °C) to be experimentally detectable.

Once more the sp atropisomer appears to adopt a chiral conformation since at −100 °C the ^{13}C lines of both the CH_2 and CH_3 ethyl carbons split into symmetric pairs of signals, the corresponding enantiomerization barrier being 9.2 kcal mol^{-1}.

Substitution of the OMe group in **4** by an OEt group yields compound **6**, which also appears to exist solely as a sp atropisomer (**6**-sp) having, at −90 °C, the H-8 shift = 9.1 ppm. At this temperature the ^{13}C spectrum displays two signals for both the CH_2 and CH_3 carbons of the ethyl groups bonded to the quaternary carbon. The corresponding enantiomerization barrier was found to be 9.7 kcal mol^{-1}, a value slightly larger than that of **4**, owing, probably, to the greater dimension of the OEt compared with the OMe substituent. Compound **6** allowed us to obtain additional proof of the chirality of the sp conformation since the lack of a symmetry plane is expected also to make the hydrogens of the OCH_2 group diastereotopic. Actually, when decoupled at the frequency of the corresponding methyl triplet, the single ^1H line of the OCH_2 hydrogens broadens and eventually splits (at −90 °C) into a typical AB pattern, the line shape analysis of which yields a $\Delta G^{\ddagger}$ value (9.7 kcal mol^{-1}) equal to that previously determined from the ^{13}C spectrum.

(e) Dimethyl-α-naphthylmethyl Methyl Ether (5) and Ethyl Ether (7). The results were essentially the same as those obtained with **4** and **6** in that only the sp atropisomers were observed at low temperature (shift of H-8 = 9.0 and 9.2 ppm, respectively, at −100 °C). These results are in agreement with calculations which predict a very large energy difference between the sp and ap atropisomers (about 5 kcal mol^{-1}). The enantiomerization barriers, measured by monitoring the appropriate diastereotopic ^{13}C methyl signals, were found to be 7.2 and 7.5 kcal mol^{-1} for **5** and **7**, respectively. In the case of **7** the same value for the enantiomerization barrier was also obtained when the diastereotopic ^1H signals of the OCH_2 hydrogens were monitored by computer simulation of the temperature dependent ABX3 pattern (the origin of such a diastereotopicity is the same as that previously reported for derivative **6**).

It should be noted that the enantiomerization barriers of **5** and **7** (which are less hindered than other derivatives having the R = Me) are about 2.5 kcal mol^{-1} lower than those measured in all the other compounds (Table 2). The same theoretical model previously employed yields computed barriers for **5**-sp and **7**-sp (6.8 and 7.0 kcal mol^{-1}, respectively) that are actually smaller, by approximately the same amount, than that computed, for instance, in **1**-sp (9.7 kcal mol^{-1}).

Conclusions

The existence of M and P conformational enantiomers, predicted by MM calculations in the atropisomers of ethers of 1-naphthylcarbinols, has been experimentally confirmed. Such enantiomers are always observed in the atropisomers having a syn periplanar (sp) structure, while the anti periplanar (ap) atropisomers, when present, prefer to adopt symmetric (thus achiral) conformations, with the notable exception of the extremely hindered *tert*-butyl derivative **1**, $MeOC(Bu^t)_2Ar$ (Ar = 1-naphthyl). In the latter compound both the **1**-sp and **1**-ap atropisomers (which can be physically separated) are chiral objects and both enantiomerization barriers were determined. It was also observed that in **1**-sp the enantiomerization is an isolated process, whereas in **1**-ap the enantiomerization is effectively correlated with the *tert*-butyl rotation. In the isopropyl derivative **2**, in addition to the atropisomer interconversion and to the enantiomerization process, the exchange of three rotamers has been also observed, generated by the restricted $C-Pr^i$ bond rotation (gear effect). Thus in compound **2** as many as four internal motions were detected and the corresponding barriers ($\Delta G^{\ddagger}$ = 13.2, 11.1, 9.7, 8.0 kcal mol^{-1}) were determined. The ethyl and methyl derivatives **4** and **5** were found to exist, on the contrary, solely as chiral sp atropisomers.

Experimental Section

Materials. Ethers **1**−**7** were prepared according to the following general procedure. To a suspension of KH (3 mmol in 5 mL of anhydrous THF) the appropriate carbinol (1 mmol in 5 mL of anhydrous THF) was added dropwise. After 10 min at room temperature, a solution of MeI (5 mmol in 3 mL of THF) was added and the solution was stirred for 1−3 h: the mixture was subsequently quenched with a NH_4Cl saturated aqueous solution and extracted with Et_2O. The organic layer was dried (Na_2SO_4) and concentrated in vacuo. Chromatography of the crude on silica gel or preparative thin-layer chromatography yielded the desired compounds. The synthesis and purification of **1-A** (sp atropisomer) was quickly carried out by keeping the temperature always below 0 °C, to avoid its interconversion into the more stable ap atropisomer **1-B**.

2,2,4,4-Tetramethyl-3-(α-naphthyl)-3-methoxypentane (1-A, sp atropisomer): mp 95 °C; ^1H NMR ($CDCl_3$, 300 MHz) 1.25 (18H, s), 3.48 (3H, s), 7.34−7.41 (4H, m), 7.74−7.80 (2H, m), 8.88 (1H, d, H8); ^{13}C NMR ($CDCl_3$, 75.5 MHz) 32.07 (CH_3), 44.13 (C,quat), 57.46 (CH_3), 94.79 (C, quat), 123.15 (CH), 124.09 (CH), 124.56 (CH), 128.37 (CH), 128.81 (CH), 130.54 (CH), 131.39 (CH), 134.5 (C, quat), 137.5 (C, quat). Anal. Calcd for $C_{20}H_{28}O$: C, 84.45; H, 9.92. Found: C, 84.37; H, 9.98.

2,2,4,4-Tetramethyl-3-(α-naphthyl)-3-methoxypentane (1-B, ap atropisomer): ^1H NMR ($CDCl_3$, 300 MHz, −10 °C) 1.3 (18 H, s), 3.45 (3H, s), 7.36−7.52 (4H, m), 7.76−7.87

(2H, m), 8.54 (1H, m, H8); ^{13}C NMR ($CDCl_3$, 75.5 MHz, −10 °C) 31.23 (CH_3), 43.60 (C, quat), 56.22 (CH_3), 95.86 (C, quat), 124.03 (CH), 124.16 (CH), 124.29 (CH), 128.61 (CH), 129.35 (CH), 129.85 (CH), 133.82 (CH), 134.46 (C, quat), 134.75 (C, quat), 138.59 (C, quat). Anal. Calcd for $C_{20}H_{28}O$: C, 84.45; H, 9.92. Found: C, 84.50; H, 9.87.

2,4-Dimethyl-3-(α-naphthyl)-3-methoxypentane (2): mp 42 °C; ^{1}H NMR ($CDCl_3$, 300 MHz) 1.02 (12H, m), 2.73 (2H, m), 3.30 (3H, s), 7.30−7.50 (4H, m), 7.60−7.90 (2H, m), 8.91 (1H, bs, H8); ^{13}C NMR ($CDCl_3$, 75.5 MHz) 18.72 (CH_3), 19.95 (CH_3), 35.06 (CH), 54.83 (CH_3), 90.14 (C, quat), 124.04 (CH), 124.64 (CH), 125.14 (CH), 128.19 (CH), 128.57 (CH), 128.86 (CH), 133.92 (C, quat), 134.71 (C, quat), 136.56 (C, quat). Anal. Calcd for $C_{18}H_{24}O$: C, 84.32; H, 9.44. Found: C, 84.39; H, 9.32.

2,6-Dimethyl-4-(α-naphthyl)-4-methoxyheptane (3): ^{1}H NMR ($CDCl_3$, 300 MHz, 40 °C) 0.58 (6H, d, J = 6.6 Hz), 0.86 (6H, d, J = 6.6 Hz), 1.63 (2H, sept, J = 6.2 Hz), 2.1 (2H, dd, J_{gem} = 14.4 Hz, J = 5.4 Hz), 2.22 (2H, dd, J_{gem} = 14.4 Hz, J = 6.3 Hz), 3.1 (3H, s), 7.3−7.6 (4H, m), 7.70−7.88 (2H, m), 8.85 (1H, d, H8); ^{13}C NMR ($CDCl_3$, 75.5 MHz; 40 °C) 24.10 (CH_3), 24.48 (CH_3), 43.77 (CH_2), 49.69 (CH_3), 84.35 (C, quat), 124.64 (CH), 128.56 (CH), 129.01 (CH), 132.33 (C, quat), 134.41 (C, quat), 140.73 (C, quat). Anal. Calcd for $C_{20}H_{28}O$: C, 84.45; H, 9.92. Found: C, 84.51; H, 9.87.

3-(α-Naphthyl)-3-methoxypentane (4): ^{1}H NMR ($CDCl_3$, 300 MHz) 0.75 (6H, t, J = 7.5 Hz), 2.11 (2H, m, J = 7.5 Hz, J_{gem} = 14.2 Hz), 2.26 (2H, m, J = 7.5 Hz, J_{gem} = 14.2 Hz), 3.00 (3H, s), 7.36−7.50 (4H, m), 7.72−7.86 (2H, m), 9.25 (1H, m); ^{13}C NMR ($CDCl_3$, 75.5 MHz) 8.05 (CH_3), 26.75 (CH_2), 49.91 (CH_3), 84.15 (C, quat), 124.44 (CH), 125.22 (CH), 125.58 (CH), 126.53 (CH), 126.89 (CH), 128.59 (CH), 128.94 (CH), 131.90 (C, quat), 134.59 (C, quat), 139.09 (C, quat). Anal. Calcd for $C_{16}H_{20}O$: C, 84.16; H, 8.83. Found: C, 84.25; H, 8.89.

2-(α-Naphthyl)-2-methoxypropane (5): ^{1}H NMR ($CDCl_3$, 300 MHz) 1.85 (6H, s), 3.1 (3H, s), 7.41−7.60 (4H, m), 7.82 (1H, dd), 7.86 (1H, m), 9.1 (1H, m); ^{13}C NMR ($CDCl_3$, 75.5 MHz), 28.52 (CH_3), 50.84 (CH_3), 79.09 (C, quat), 124.74 (CH), 125.00 (CH), 125.32 (CH), 125.53 (CH), 125.72 (CH), 126.96 (CH), 128.77 (CH), 131.66 (C, quat), 134.52 (C, quat), 140.41 (C, quat). Anal. Calcd for $C_{14}H_{16}O$: C, 83.96; H, 8.05. Found: C, 84.05; H, 8.13.

3-(α-Naphthyl)-3-ethoxypentane (6): ^{1}H NMR ($CDCl_3$, 300 MHz) 0.72 (6H, t, J = 7.4 Hz), 1.08 (3H, t, J = 7.1 Hz), 2.08 (2H, m, J = 7.4 Hz, J_{gem} = 14.2 Hz), 2.23 (2H, m, J = 7.4 Hz, J_{gem} = 14.2 Hz), 3.06 (2H, q, J = 7.1 Hz), 7.34−7.50 (4H, m), 7.70−7.84 (2H, m), 9.08 (1H, m); ^{13}C NMR ($CDCl_3$, 75.5 MHz) 8.12 (CH_3), 15.69 (CH_3), 27.02 (CH_2), 57.37 (CH_2), 83.57 (C, quat), 124.48 (CH), 125.27 (CH), 126.23 (CH), 127.11 (CH), 128.52 (CH), 128.94 (CH), 131.90 (C, quat), 134.59 (C, quat), 139.80 (C, quat). Anal. Calcd for $C_{17}H_{22}O$: C, 84.25; H, 9.15. Found: C, 84.32; H, 9.21.

2-(α-Naphthyl)-2-ethoxypropane (7): ^{1}H NMR ($CDCl_3$, 300 MHz) 1.08 (3H, t, J = 7.0 Hz), 1.8 (6H, s), 3.15 (2H, q, J = 7.0 Hz), 7.3−7.52 (4H, m), 7.7−7.9 (2H, m), 9.25 (1H, m); ^{13}C NMR ($CDCl_3$, 75.5 MHz) 15.87 (CH_3), 28.91 (CH_3), 58.39 (CH_2), 78.56 (C, quat), 124.64 (CH), 124.69 (CH), 125.29 (CH), 125.34 (CH), 127.13 (CH), 128.57 (CH), 128.78 (CH), 131.56 (C, quat), 134.50 (C, quat), 141.10 (C, quat). Anal. Calcd for $C_{15}H_{18}O$: C, 84.07; H, 8.47. Found: C, 84.17; H, 8.40.

NMR Measurements. The variable temperature NMR spectra were recorded either at 300 (^{1}H) and 75.5 MHz (^{13}C) or at 400 (^{1}H) and 100.6 MHz (^{13}C). The ^{1}H low-temperature spectrum of **2** was also obtained at 600 MHz, for which we thank the Highfield NMR Laboratory of the University of Florence and Mr. M. Lucci for assistance.

The computer simulation of the line shape was performed by a computer program[21] based on DNMR6 routines, and the best fit was visually judged by superimposing the plotted and experimental traces. The samples for measurements below −100 °C were prepared by connecting the NMR tubes, containing a small amount of a deuterated compound (C_6D_6 or CD_2Cl_2) for locking purpose, to a vacuum line and condensing the gaseous solvents (CHF_2Cl, $CBrF_3$) with liquid nitrogen. The tubes were then sealed in vacuo and introduced in the precooled probe of the spectrometer. The difference NOE measurements were carried out in solutions, purged from dissolved oxygen using a nitrogen stream, by presaturating the signal for about 10 s and acquiring the spectrum with the decoupler turned off. The various lines of the multiplets were saturated by cycling the irradiation frequencies about 40 times. A program which acquires the difference between the two FID's (that being irradiated and that acquired with the irradiation frequency kept away from any signal) was employed (128 or 256 scans were, usually, accumulated). The control spectrum was subsequently acquired with half the number of scans.

X-ray Diffraction. Crystal data for $C_{20}H_{28}O$, **1A**: M = 284.42, monoclinic, space group $P2_1$, a = 8.010(4), b = 15.782(4), and c = 20.151(4) Å, β = 98.96(3)°, U = 2516(1) Å^3, Z = 6, D_c = 1.13 mg/m^3, $F_{(000)}$ = 936, λ = 0.710 69 Å, T = 298 K, μ(Mo K)α = 0.067 mm^{-1}. The unit cell contains three independent molecular units, two of these having opposite chirality. Data were collected on an Enraf-Nonius CAD-4 diffractometer using graphite monochromatic Mo−Kα radiation, $\omega/2\theta$ scan mode, range 2.57° < θ < 24.98°. The unit cell parameters were determined by least-squares refinement on diffractometer angles for 25 automatically centered reflections 7.35° < θ < 14.78°. Of 4593 independent reflections [R(int) = 0.0134], 2880 having $I > 2\sigma(I)$ were considered observed. The structure was solved by direct methods and refined by full-matrix least squares on F^2, using the SHELX program packages.[22] In refinements were used weights according to the scheme $w = 1/[\sigma^2(F_o^2) + (0.1061P)^2 + 2.2313P]$, where $P = (F_o^2 + 2F_c^2)^3$. The hydrogen atoms were located by geometrical calculation and refined using a "riding" model. The final agreement indices were R = 0.0698 and wR = 0.1835. Goodness of fit on F^2 = 1.018. Largest difference peak and hole were 0.544 and −0.328 Å^{-3}.

Acknowledgment. Thanks are due to Dr. J. E. Anderson, University College, London, UK, for helpful comments and for hosting one of us (A.M.) to use the 400 MHz spectrometer. We are also indebted to Miss L. D'Adamo (University of Bologna) for helpful technical assistance. Financial support was obtained from the Ministry of the University and Scientific Research (MURST), from the National Research Council (CNR, Rome), and from the University of Bologna (Funds for selected research topics 1995−1997).

Supporting Information Available: Listing of fractional atomic coordinates, thermal parameters, relevant atomic distances, and observed and calculated structure factors for derivative **1A** and difference NOE spectra for derivatives **1-A** and **1-B** (12 pages). This material is contained in libraries on microfiche, immediately follows this article in the microfilm version of the journal, and can be ordered from the ACS; see any current masthead page for ordering information.

JO9804801

(21) Courtesy of Professor F. Gasparrini, University La Sapienza, Rome.

(22) Sheldrick, G. M. SHELX-86, *Acta Crystallogr.* **1990**, *A46*, 467. SHELX-93, University of Gottingen, Germany, 1993.